

# Salinity Sensor



**Prepared by:**

Cameron Clark Department of Electrical Engineering  
University of Cape Town

**Prepared for:**

Justin Pead  
Department of Electrical Engineering  
University of Cape Town

October 9, 2024

Submitted to the Department of Electrical Engineering at the University of Cape Town in partial fulfilment of the academic requirements for a Bachelor of Science degree in Mechatronics

**Keywords:** Salinity, Sensor, Conductivity, Temperature, Water, Measurement, Electronics, PCB

# Declaration

1. I know that plagiarism is wrong. Plagiarism is to use another's work and pretend that it is one's own.
2. I have used the IEEE convention for citation and referencing. Each contribution to, and quotation in, this report .... from the work(s) of other people has been attributed and has been cited and referenced. Any section taken from an internet source has been referenced to that source.
3. This report .... is my own work and is in my own words (except where I have attributed it to others).
4. I have not paid a third party to complete my work on my behalf. My use of artificial intelligence software has been limited to ..... (specify precisely how you used AI to assist with this assignment, and then give examples of the prompts you used in your first appendix).
5. I have not allowed and will not allow anyone to copy my work with the intention of passing it off as his or her own work.
6. I acknowledge that copying someone else's assignment or essay, or part of it, is wrong, and declare that this is my own work



October 9, 2024

---

Cameron Clark

---

Date

# Acknowledgements

# Abstract

# Contents

|                                                                    |             |
|--------------------------------------------------------------------|-------------|
| <b>List of Figures</b>                                             | <b>vii</b>  |
| <b>Abbreviations</b>                                               | <b>viii</b> |
| <b>1 Introduction</b>                                              | <b>1</b>    |
| 1.1 Background . . . . .                                           | 1           |
| 1.2 Objectives . . . . .                                           | 1           |
| 1.3 System Requirements . . . . .                                  | 1           |
| 1.4 Scope & Limitations . . . . .                                  | 2           |
| 1.5 Report Outline . . . . .                                       | 2           |
| <b>2 Literature Review</b>                                         | <b>3</b>    |
| 2.1 A Brief History of Salinity . . . . .                          | 3           |
| 2.2 Salinity Measurement Methods . . . . .                         | 4           |
| 2.2.1 Salinity from Chlorinity . . . . .                           | 4           |
| 2.2.2 Salinity from Conductivity . . . . .                         | 4           |
| 2.2.3 Salinity from Density . . . . .                              | 5           |
| 2.2.4 Salinity from Microwave Radiation . . . . .                  | 5           |
| 2.2.5 Salinity from Refractive Index . . . . .                     | 6           |
| 2.2.6 Salinity from Interferometry . . . . .                       | 6           |
| 2.2.7 Salinity from Electromagnetic Induction . . . . .            | 6           |
| 2.3 Salinity Measurement Devices using Conductivity . . . . .      | 7           |
| <b>3 Theory Development</b>                                        | <b>8</b>    |
| 3.1 The Calculation of Salinity From Conductivity . . . . .        | 8           |
| 3.2 Electrical Characteristics of Salt Water . . . . .             | 10          |
| 3.3 Electrical Fringing in Conductive Materials . . . . .          | 10          |
| <b>4 Design</b>                                                    | <b>11</b>   |
| 4.1 Salinity Measurement Method . . . . .                          | 11          |
| 4.2 Conductivity Probe Material . . . . .                          | 11          |
| 4.3 Conductivity Probe Design . . . . .                            | 12          |
| 4.4 Resistance Measurement Method . . . . .                        | 13          |
| 4.5 Circuit Overview . . . . .                                     | 13          |
| 4.6 Salinity Calculation and Display . . . . .                     | 15          |
| 4.7 Temperature and Depth Measurement . . . . .                    | 16          |
| 4.8 Printed Circuit Board (PCB) Assembly and Corrections . . . . . | 16          |
| 4.9 Salinometer Code . . . . .                                     | 16          |

|                                             |           |
|---------------------------------------------|-----------|
| 4.10 Controller Code . . . . .              | 17        |
| <b>5 Salinometer Evaluation and Testing</b> | <b>18</b> |
| 5.1 DAC Voltage Range . . . . .             | 19        |
| 5.2 ADC Accuracy . . . . .                  | 21        |
| 5.3 Calibration Resistance . . . . .        | 21        |
| 5.4 Resistance Measuring Accuracy . . . . . | 21        |
| <b>6 Conclusions</b>                        | <b>24</b> |
| <b>7 Recommendations</b>                    | <b>25</b> |
| <b>Bibliography</b>                         | <b>26</b> |

# List of Figures

|     |                                                                                                                                                                                       |    |
|-----|---------------------------------------------------------------------------------------------------------------------------------------------------------------------------------------|----|
| 2.1 | Histogram showing the volume of ocean water relative to temperature and salinity bins.<br>The highest peak corresponds to a volume of 26 million cubic kilometres of ocean water [1]. | 3  |
| 2.2 | Global salinity map generated using satellite data [2]. . . . .                                                                                                                       | 5  |
| 4.1 | The gold electrode PCB design. . . . .                                                                                                                                                | 13 |
| 4.2 | A simplified representation of the resistance measuring circuit. . . . .                                                                                                              | 14 |
| 4.3 | A simplified representation of the resistance measurement circuit using the gold electrodes<br>with the fringe guard. . . . .                                                         | 15 |
| 5.1 | The input voltage versus the output voltage of the Digital to Analogue Converter (DAC)<br>with no load. . . . .                                                                       | 20 |
| 5.2 | The input voltage versus the output voltage of the DAC with a load of $100\Omega$ . . . . .                                                                                           | 20 |
| 5.3 | The voltage output by the DAC measured by a multimeter versus measured by the<br>Analogue to Digital Converter (ADC). . . . .                                                         | 21 |
| 5.4 | The resistance measuring test. . . . .                                                                                                                                                | 22 |
| 5.5 | The resistance measuring test using the correction equation. . . . .                                                                                                                  | 22 |

# Abbreviations

**‰** Parts Per Thousand

**ADC** Analogue to Digital Converter

**CTD** Conductivity, Temperature, Depth

**DAC** Digital to Analogue Converter

**EMI** Electromagnetic Interference

**ENIG** Electroless Nickel Immersion Gold

**FPU** Floating Point Unit

**PCB** Printed Circuit Board

**ppm** parts per million

**PSU** Practical Salinity Units

**SST** Sea Surface Temperature



# Chapter 1

## Introduction

Antarctica is the coldest continent on Earth covered in a vast sheet of ice that contains about 30 million cubic kilometres of ice [3] which is about 60% of the world's fresh water. This ice sheet is currently melting at an increasing rate due to global warming and other factors and scientists are trying to understand why. One of the methods being used to analyse sea ice is drilling ice cores and analysing the ice for various properties from the concentration of gases to the concentration of dust particles. One of the properties that is currently difficult to analyse is the salinity of the melted and solid sea ice. This project aims to develop a system that can measure the salinity of the melted sea ice at the bottom of the ice cores mentioned.

### 1.1 Background

more about the project sea ice and what this analysis will help with.

### 1.2 Objectives

The objectives of this project are to create a device that is able to measure the salinity of sea ice at the bottom of ice cores. The device should be able to measure the salinity of the ice in harsh conditions and cold environments that will be present in Antarctica. The device should also be able to measure the salinity of the ice in a non-destructive manner so that the ice core can be used for other analysis after the salinity has been measured.

### 1.3 System Requirements

Lorem ipsum dolor sit amet, consectetur adipiscing elit. Ut purus elit, vestibulum ut, placerat ac, adipiscing vitae, felis. Curabitur dictum gravida mauris. Nam arcu libero, nonummy eget, consectetur id, vulputate a, magna. Donec vehicula augue eu neque. Pellentesque habitant morbi tristique senectus et netus et malesuada fames ac turpis egestas. Mauris ut leo. Cras viverra metus rhoncus sem. Nulla et lectus vestibulum urna fringilla ultrices. Phasellus eu tellus sit amet tortor gravida placerat. Integer sapien est, iaculis in, pretium quis, viverra ac, nunc. Praesent eget sem vel leo ultrices bibendum. Aenean faucibus. Morbi dolor nulla, malesuada eu, pulvinar at, mollis ac, nulla. Curabitur auctor semper nulla. Donec varius orci eget risus. Duis nibh mi, congue eu, accumsan eleifend, sagittis quis, diam. Duis eget orci sit amet orci dignissim rutrum.

## 1.4 Scope & Limitations

The scope of this project includes the design and development of a device that can measure the salinity of sea ice at the bottom of ice cores. It includes the calibration of the devices, calculations for it, and establishing the accuracy of the device. The scope does not include the capture and analysis of the data from the device.

It is limited to performing in the conditions of Anartica and measureing melted sea ice. It is limited by a budget of R2000 for the full design and development of the device.

## 1.5 Report Outline

Lorem ipsum dolor sit amet, consectetur adipiscing elit. Ut purus elit, vestibulum ut, placerat ac, adipiscing vitae, felis. Curabitur dictum gravida mauris. Nam arcu libero, nonummy eget, consectetur id, vulputate a, magna. Donec vehicula augue eu neque. Pellentesque habitant morbi tristique senectus et netus et malesuada fames ac turpis egestas. Mauris ut leo. Cras viverra metus rhoncus sem. Nulla et lectus vestibulum urna fringilla ultrices. Phasellus eu tellus sit amet tortor gravida placerat. Integer sapien est, iaculis in, pretium quis, viverra ac, nunc. Praesent eget sem vel leo ultrices bibendum. Aenean faucibus. Morbi dolor nulla, malesuada eu, pulvinar at, mollis ac, nulla. Curabitur auctor semper nulla. Donec varius orci eget risus. Duis nibh mi, congue eu, accumsan eleifend, sagittis quis, diam. Duis eget orci sit amet orci dignissim rutrum.

# Chapter 2

## Literature Review

### 2.1 A Brief History of Salinity

The most commonly understood definition of salinity relates it to the total amount of dissolved *salts* in a solution, however, salinity's definition has had several more complex iterations over the years. One of the first definitions of salinity was the total amount of dissolved *material* in grams in one kilogram of water [4]. This is a dimensionless quantity that was expressed in [Parts Per Thousand \(‰\)](#) or  $g.kg^{-1}$  where most ocean's salinity fell between 34.60‰ and 34.80‰ as shown in Figure 2.1.

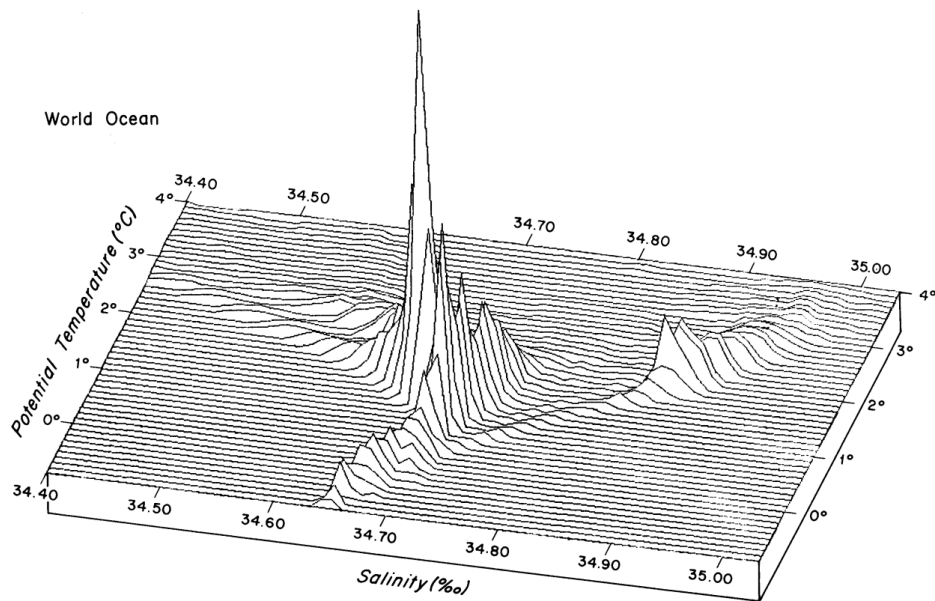


Figure 2.1: Histogram showing the volume of ocean water relative to temperature and salinity bins. The highest peak corresponds to a volume of 26 million cubic kilometres of ocean water [1].

The problem with this definition of salinity lay with its testability. Trying to obtain the mass of the dissolved material through evaporation removed certain compounds making this method inaccurate [5] and other methods of isolating the mass of the dissolved material had similar issues. Salinity needed to be redefined in a way that was easily and reliably testable which led to the next definition of salinity which related salinity related it to the amount of chlorine present in the water, or the chlorinity of the water and in 1969, salinity was redefined to be directly proportional to the chlorinity of the water [4]. The calculation of salinity from chlorinity is further discussed in Section 2.2.1.

Around the same time as the salinity-chlorinity relationship was established, oceanographers had begun experimenting with using conductivity to measure salinity. Conductivity was found to be more precise and significantly easier to measure than the titration required to measure chlorinity [6]. In 1978, the Practical Salinity Scale was established and salinity was redefined to be related to conductivity which is the current definition of salinity[6]. This relationship also included terms for temperature and depth as these affect the conductivity of an electrolyte solution [7].

The Practical Salinity Scale uses its own dimensionless units of salinity which are not interchangeable with ‰ in the current definition of salinity. Although the Practical Salinity Scale is sometimes given in **Practical Salinity Units (PSU)**, it is more technically correct to refer to it as a certain Practical Salinity ‘on the Practical Salinity Scale PSS-78’ [6]. The calculation of salinity from conductivity is further discussed in Section 3.1.

## 2.2 Salinity Measurement Methods

Salinity has had a long history of being measured using a variety of methods with varying degrees of accuracy. Currently, the most common method of measuring salinity is through the use of a **Conductivity, Temperature, Depth (CTD)** instrument, but there are several other methods to achieve this, most of which have been developed over the last 3 decades.

### 2.2.1 Salinity from Chlorinity

The chemical composition of ocean water with a salinity of 35‰ contains 19.35‰ of Chlorine and 10.77‰ of Sodium with the next most common ions only accounting for just above 3‰ of the total dissolved solids in the water [8]. This allowed oceanographers to estimate that the salinity of ocean water was directly proportional to the amount of chlorine in the water. The chlorinity of a solution had an established definition which was ‘the mass of silver required to precipitate completely the halogens in 0.328 523 4kg of the ocean-water sample’ [9] which could be tested using titration. In 1969, an accurate relationship between these was established by Reference [9] and thus salinity  $S$  was redefined using chlorinity  $Cl$  as shown in Equation 2.1.

$$S(\text{‰}) = 1.80655 \times Cl(\text{‰}) \quad (2.1)$$

*accuracy achieved?, device?, limitations?*

### 2.2.2 Salinity from Conductivity

The conductivity of a liquid is a measure of the ability of the water to conduct an electrical current which is related to the number of free electrons present in the liquid which is in turn related to the number of ions present in the liquid. In the case of salt water, the ions present are from the dissolved material which is what salinity was previously defined on. The relationship between salinity and conductivity takes into account all the ions present in the water and thus was a more apt measure of salinity than chlorinity which is why salinity was redefined in terms of salinity. Calculating salinity from conductivity requires several equations as it needs correction for both temperature and pressure. These equations are further discussed in Section 3.1. *accuracy achieved?, device?, limitations?*

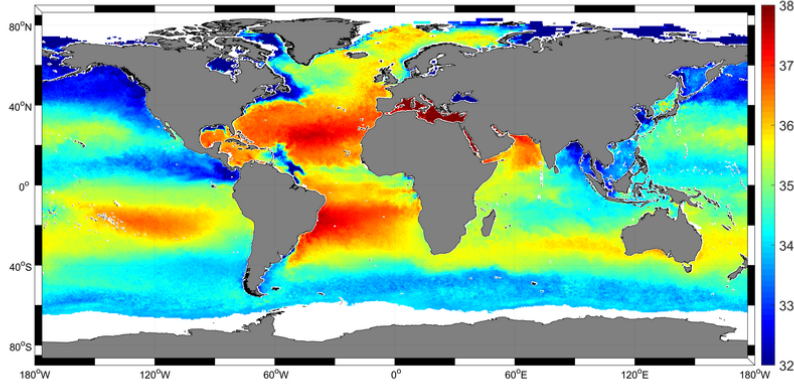


Figure 2.2: Global salinity map generated using satellite data [2].

### 2.2.3 Salinity from Density

The density of pure water varies with temperature and is considered to be approximately  $1000 \text{ kg.m}^{-3}$  at  $4^\circ\text{C}$  [10]. Adding denser materials to the water will intuitively increase its density and this change can be measured to determine the quantity of dissolved material in the water which relates to salinity. The relationship between salinity and density could be approximated to be linear as shown in Equation 2.2 where  $\rho$  is the density of the water,  $\rho_0$  is the density of pure water,  $k$  is a proportionality constant, and  $S$  is the salinity of the water [11][12].

$$\rho = \rho_0(1 + kS) \quad (2.2)$$

This relationship was further refined to include temperature into the relationship [13]. Reference [13] claimed that density was a better measure of salinity than conductivity as the standard potassium chloride solution used to calibrate the CTDs meters did not account for non-conductive material commonly present in salt water while the density of the water did, however salinity remained defined in terms of conductivity. *accuracy achieved?, device?, limitations?*

### 2.2.4 Salinity from Microwave Radiation

The electromagnetic spectrum interacts with salt water in unique ways, scattering, refracting and reflecting when it comes in contact with the water and any material dissolved in the water. Different temperature molecules in the water scatter electromagnetic waves differently and the pressure of the water can also affect this, but the most significant effect on the microwave radiation is from the presence of dissolved material in the water [14].

Microwave radiation is one section of the electromagnetic spectrum that take advantage of this fact to measure salinity [14]. The relationship between salinity and microwave radiation is complex but since microwave radiation does not require direct contact with the water, it is possible to measure the salinity of a sample of water from a far distance including from space [15]

This has allowed for the development of satellites that can measure the salinity which have been used to develop global salinity maps as shown in Figure 2.2. The data measured using this method is reported to be accurate to within 0.1 on the Practical Salinity Scale PSS-78 [16], but this method requires multiple different readings to be taken in order to account for the different factors that affect

the microwave radiation including [Sea Surface Temperature \(SST\)](#), surface air pressure, surface air temperature, faraday rotation, and surface wind speed [16].

### 2.2.5 Salinity from Refractive Index

The second measurement method that takes advantage of the electromagnetic spectrum interaction with salt water uses the visible light spectrum to measure the refractive index of the water. The relationship between salinity and refractive index is complex requiring a 27 term equation which includes the effect of pressure and temperature on the water's refractive index. The refractive index equation is defined a range of  $500 - 700nm$  in wave length,  $0 - 30^{\circ}C$  in temperature, and  $0 - 40$  on the Practical Salinity Scale PSS-78, and  $0 - 11000dbar$  in pressure. The equation holds an accuracy of  $0.4 - 80$  [parts per million \(ppm\)](#) on the Practical Salinity Scale PSS-78, decreasing with increasing pressure. [17]

A refractometer is the device that is used to measure the refractive index of the water, and due to only needing a small amount of the sample, these devices can be quite compact. A few researches have developed compact refractometers, the notable ones of which have dimensions of  $22.5mm \times 22.5mm \times 120mm$  [18] and  $40mm \times 40mm \times 70mm$  [19] which achieved accuracies of 2 and 83 ‰ on the Practical Salinity Scale PSS-78 respectively.

### 2.2.6 Salinity from Interferometry

The last measurement methods that takes advantage of the electromagnetic spectrum interaction with salt water is interferometry. Interferometry involves generating two identical light waves one the visible spectrum and then passing one through the sample and then comparing the two waves to identify the phase shift and gain. These measurements can be used to identify the salinity of a sample of salt water [20].

This method has varying implementation with varying results with Reference [21] reporting accuracies down to 0.001 on the Practical Salinity Scale PSS-78 using a Michelson interferometer which other researches have reported other accuracies using different methods [22][23][24]. The refractometer does have the disadvantage of being large instrument as the mirrors required to direct the light waves require space and precise alignment making this a difficult method to implement in a compact device.

### 2.2.7 Salinity from Electromagnetic Induction

Similarly to conductivity, the magnetic permeability of a liquid is related to the number of ions present in the liquid. The more ions present in the liquid, the stronger the magnetic field that can be generated by the liquid which increases the magnetic permeability of the liquid which is related to the total dissolved solids in salt water's case [25].

There are several methods of measuring the magnetic permeability of a liquid that all involve inducing a magnetic field in the liquid and then measuring its response. These methods all have the advantage of not requiring direct contact with the salt water to make the measurement which allows for the sample to remain undisturbed unlike the conductivity method [26]. This method has not been fully investigated however the equipment that is required to measure the magnetic permeability of a liquid

is relatively large and requires a lot of power to operate which makes it difficult to implement in a compact device for use in remote environments.

## **2.3 Salinity Measurement Devices using Conductivity**

## Chapter 3

# Theory Development

### 3.1 The Calculation of Salinity From Conductivity

Salinity meters that use electrical conductivity are commonly known as **CTDs**. As depth is a measurement derived from pressure, CTP is the preferred designation when performing calculations. This allows for the conductivity of a sample of water to be denoted by  $C(S, T, p)$  where conductivity is a function of salinity  $S$ , temperature  $T$ , and pressure  $p$  which is the convention in oceanography [6]. Pressure in the salinity equation is taken relative to sea level where  $p = 0\text{dbar}$  is equivalent to an absolute pressure of  $P = 101\,325\text{Pa}$ . Using decibars (dbar) for pressure is a common practice in oceanography as it is a unit of pressure that is equal to roughly one meter of water depth [27].

The Practical Salinity Scale defines Practical salinity  $S_p$  in terms of a conductivity ratio  $K_{15}$  which is the conductivity of a sample of water at a temperature of  $15^\circ\text{C}$  and a pressure equal to one standard atmosphere divided by the conductivity of a standard potassium chloride solution at the same temperature and pressure. The standard potassium chloride solution is  $32.4356\text{g}$  of  $KCl$  dissolved in  $1.000\text{kg}$  of water and when the ratio between the conductivity of a sample of water and the standard solution, or  $K_{15}$ , equals 1 the Practical Salinity  $S_p$  is, by definition, 35.

When  $K_{15}$  is not equal to 1, the Practical Salinity  $S_p$  can be calculated using the PSS-78 equation shown in Equation 3.1.

$$S_p = \sum_{i=0}^5 a_i (K_{15})^{i/2} \quad \text{where} \quad K_{15} = \frac{C(S_p, 15^\circ\text{C}, 0)}{C(35, 15^\circ\text{C}, 0)} \quad (3.1)$$

All the coefficients for the salinity-conductivity equations, including  $a_i$ , are given in Table 3.1.

To calculate the salinity of a sample of water that is not at  $15^\circ\text{C}$  and  $0\text{dbar}$ , the conductivity ratio of the sample can be expanded into the product of three ratios which are labelled  $R_p$ ,  $R_t$ , and  $r_t$  respectively. The conductivity measurement taken in the field  $C(S_p, t, p)$  is related to the conductivity of the standard solution  $C(35, 15^\circ\text{C}, 0)$  which the device is calibrated with and is represented by  $R$  in Equation 3.2. [28]

$$R = \frac{C(S_p, t, p)}{C(35, 15^\circ\text{C}, 0)} = \frac{C(S_p, t, p)}{C(S_p, t, 0)} \cdot \frac{C(S_p, t, 0)}{C(35, t, 0)} \cdot \frac{C(35, t, 0)}{C(35, 15^\circ\text{C}, 0)} = R_p R_t r_t \quad (3.2)$$

*check* In order to calculate the salinity of the sample  $R_t$  must be found which takes a similar for to



### 3.1. The Calculation of Salinity From Conductivity

$K_{15}$ .  $r_t$  is first calculated using the temperature of the sample

$$r_t = \sum_{i=0}^4 c_i t^i \quad (3.3)$$

following which  $R_p$  is calculated using the sample's pressure  $p$ , temperature  $t$  and conductivity ratio  $R$ ,

$$R_p = 1 + \frac{\sum_{i=1}^3 e_i p^i}{1 + d_1 t + d_2 t^2 + R[d_3 + d_4 t]} \quad (3.4)$$

and finally  $R_t$  is calculated using  $r_t$ ,  $R_p$  and  $R$ .

$$R_t = \frac{R}{R_p r_t} \quad (3.5)$$

Note that for a sample temperature of  $15^\circ\text{C}$  and pressure of  $0\text{dbar}$ ,  $r_t$  and  $R_t$  both equal 1 which leaves  $R_t$  equal to  $R$  and thus Equation 3.1 can be used to calculate the Practical Salinity  $S_p$ . For temperatures other than  $15^\circ\text{C}$ , the Practical Salinity  $S_p$  can be calculated using Equation 3.6 where  $k = 0.0162$ . [28]

$$S_p = \sum_{i=0}^5 a_i (R_t)^{i/2} + \frac{t - 15}{1 + k(t - 15)} \sum_{i=0}^5 b_i (R_t)^{i/2} \quad (3.6)$$

Table 3.1: Coefficients for the PSS-78 equations [28].

| $i$ | $a_i$   | $b_i$   | $c_i$                    | $d_i$                  | $e_i$                   |
|-----|---------|---------|--------------------------|------------------------|-------------------------|
| 0   | 0.0080  | 0.0005  | $6.766097 \cdot 10^{-1}$ |                        |                         |
| 1   | -0.1692 | -0.0056 | $2.00564 \cdot 10^{-2}$  | $3.426 \cdot 10^{-2}$  | $2.070 \cdot 10^{-5}$   |
| 2   | 25.3851 | -0.0066 | $1.104259 \cdot 10^{-4}$ | $4.464 \cdot 10^{-4}$  | $-6.370 \cdot 10^{-10}$ |
| 3   | 14.0941 | -0.0375 | $-6.9698 \cdot 10^{-7}$  | $-4.215 \cdot 10^{-3}$ | $3.989 \cdot 10^{-15}$  |
| 4   | -7.0261 | 0.0636  | $1.0031 \cdot 10^{-9}$   | $-3.107 \cdot 10^{-3}$ |                         |
| 5   | 2.7081  | -0.0144 |                          |                        |                         |

Note that the coefficients  $a_i$  precisely sum to 35 such that the Practical Salinity  $S_p$  is 35 when  $K_{15}$  or  $R_t = 1$  as per Equation 3.1 and Equation 3.6. Additionally, the coefficients  $b_i$  precisely sum to 0 such that the Practical Salinity  $S_p$  does not depend on the temperature of the water when  $R_t = 1$  as per Equation 3.6. [28]

Equation 3.1 to Equation 3.6 are valid for  $2 < S_p < 42$  and  $-2^\circ\text{C} < t < 35^\circ\text{C}$  and  $0\text{dbar} < p < 10\,000\text{dbar}$  [28]. The range for salinity has been extended using estimations by Reference [29] for  $0 < S_p < 2$  and Reference [30] for  $42 < S_p < 50$ .

The temperatures used in Equation 3.1 to Equation 3.6 are on the IPTS-68 scale [31] and have not been corrected to the currently used ITS-90 scale [32]. In order to correctly calculate the salinity, the temperatures should be converted to the IPTS-68 scale using the equation  $t_{68} = 1.00024t_{90}$  before

calculating salinity [\[32\]](#).

### **3.2 Electrical Characteristics of Salt Water**

PSU vs TSD vs conductivity vs resistivity, salinity equation, capacitance of salt water, non-constant conductivity vs voltage.

### **3.3 Electrical Fringing in Conductive Materials**

# Chapter 4

## Design

*dac buffer*

### 4.1 Salinity Measurement Method

*help* Of the available methods for measuring salinity, the most common method used in oceanography is the conductivity method. This is because conductivity of salt water is the easiest to repeatably measure and provides the most consistent accuracy. Information on other methods can be found in the literature review.

One of the most common methods of measuring conductivity of a liquid is to measure the resistance between two electrodes or probes in the liquid and use that to determine its conductivity. The shape and material of the probes are an important factor which affect the measurement accuracy and drift as well as the ease of calculation from resistance to conductivity.

### 4.2 Conductivity Probe Material

Ideal probes for measuring conductivity in salt water need to have zero resistance, infinite corrosion resistance and be able to confine the electrical current in the water to a specific volume. The zero resistance will allow the resistance that it measured to be entirely due to the water, although most conductive materials have a conductivity in the order of  $10^8 S/m$  which causes negligible resistance compared to water which has a conductivity range of  $0 - 5 S/m$ . The infinite corrosion resistance will allow the probes to last indefinitely in the highly corrosive salt water. The confinement of the electrical current allows for an easier calculation of the conductivity  $\rho$  from resistance  $R$  if the cross-sectional area  $A$  and length  $l$  of the water between the probes is known as shown by Equation 4.1.

$$\rho = \frac{RA}{l} \quad (4.1)$$

There are several metals known for their corrosion resistance which are used in corrosive environments including marine environments. The most abundant of these are aluminium and stainless steel, followed by nickel and copper alloys, such as Monel or brass, and finally titanium. Additionally, the precious metals gold, silver and platinum are also known for their exceptional corrosion resistance which exceeds the aforementioned metals, although they are significantly more expensive.

The choice of material aimed at using materials with the highest corrosion resistance while still choosing materials that were attainable and within this project's budget. Titanium is the most corrosive resistant

of the non-precious metals and has an acceptable resistivity of  $4.5 \cdot 10^{-7} \Omega \cdot m$  which is about 25 times that of copper. Titanium wire was available through off-cuts from a project being conducted by the Chemical Engineering Department of the University of Cape Town, and thus it was possible to use this material for the electrodes.

Of the precious metals, gold is one of the most accessible as it is a common material used in [Printed Circuit Boards \(PCBs\)](#) manufacturing primarily because of its high corrosion resistance while it maintains a low resistivity of  $2.44 \cdot 10^{-8} \Omega \cdot m$  similar to copper. [Electroless Nickel Immersion Gold \(ENIG\) PCB](#) manufacturing is a process where nickel followed by gold are deposited onto the copper of the [PCB](#) using chemical reactions. While this process is expensive, it is affordable within this project's budget and made gold a possible material for the electrodes.

Gold and titanium were both used as electrodes for this project due to their high corrosion resistance, conductivity and availability.

### 4.3 Conductivity Probe Design

Gold electrodes made using the [ENIG PCB](#) manufacturing process were chosen to be the primary electrodes for the device. The high corrosion resistance and conductivity of gold were advantageous, and the [PCB](#) allowed the probes to be made with a known area and length of the water between the probes.

Some scientific papers that attempt to measure salinity have an uncertainty on whether salt water has a constant resistivity relative to the voltage applied to it or not. In order to verify this, the resistance of the water between the probes needed to be measured at different voltages while other factors were kept constant which necessitated close attention to the fringing effect of the electrical current between the probes. Thus, wide flat pads were used on the [PCB](#) probes, and they were placed them close together to reduce the amount of current fringing allowing for a more accurate calculation of the conductivity. To further reduce the fringing, a fringe guard was added to the probes which consisted of a pad that outlined the main conductivity pads that repeated the same voltage as the main pads using an op-amp which would allow for the fringing to be taken up by the fringe guard and not affect the resistance measurement.

The dimensions of the gold electrodes were chosen somewhat arbitrarily with the pads having a large area while being placed relatively close together to reduce the fringing but not too close to prevent water from flowing between the pads. Additionally, the aim was to keep the resistance between the pads low to lower the amount of voltage required to generate a current through the water thus further reducing the fringing. The gold electrodes were designed with a  $20mm \times 20mm$  pad area with a  $2mm$  wide fringe guard surrounding the majority of the pad and were spaced  $10mm$  apart as shown in [Figure 4.1](#). This gave a resistance of  $3.75\Omega$  to  $6.25\Omega$  between the gold electrodes for salinities of 40 to 25 on the practical salinity scale respectively.

The titanium electrodes are substantially simpler and cheaper than the gold electrodes and would be the preferred electrodes if the fringing effect could be accounted for. Provided the testing with the gold electrodes is able to prove a constant resistance-voltage relationship, the fringing effect between the

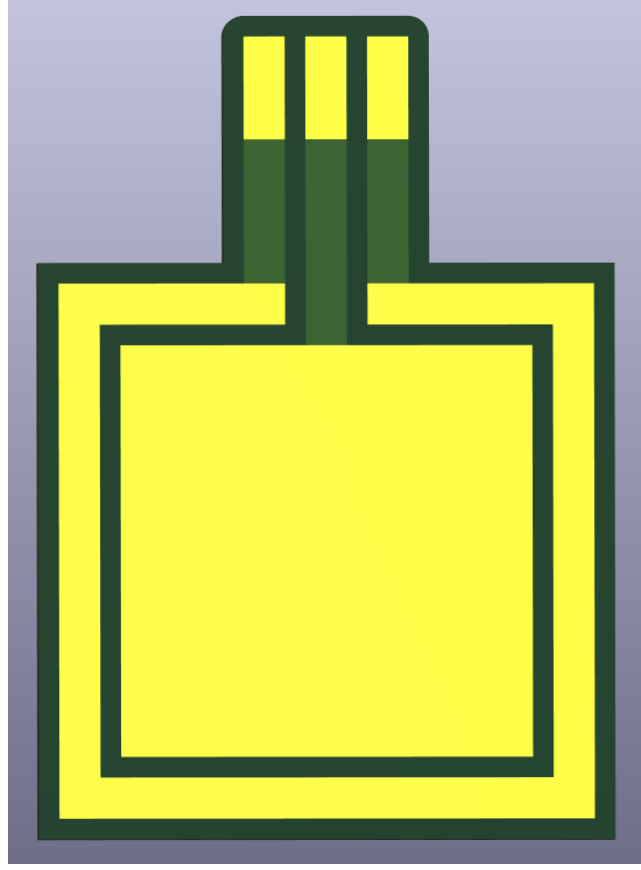


Figure 4.1: The gold electrode PCB design.

titanium electrodes could be measured and accounted for allowing for them to be used as the primary electrodes in a future iteration of the device. The titanium wire that was available for this project was  $1mm$  in diameter and in order to account for the unknown resistance between the electrodes, the design allowed for an adjustable spacing between the electrodes and adjustable electrode length.

## 4.4 Resistance Measurement Method

The most common and practical method of measuring resistance is to use a resistor divider circuit. Current meters are also used to measure resistance, but most of them use the same principle of a resistor divider circuit to determine the current. This project chose to use a large  $R_1$  in series with the electrodes such that the voltage between the probes would be lower which would further reduce the fringing effect. The measurement taken from the voltage divider was then amplified by a factor of 11 to increase the resolution of the measurement.

## 4.5 Circuit Overview

*additional advantage : will never short circuit*

Figure 4.2 shows a simplified overview of the resistance measuring circuit that was used in this project. The voltage driving the resistor divider was provided by a [Digital to Analogue Converter \(DAC\)](#) such that the voltage could be varied and the resistance-voltage relationship could be determined for the

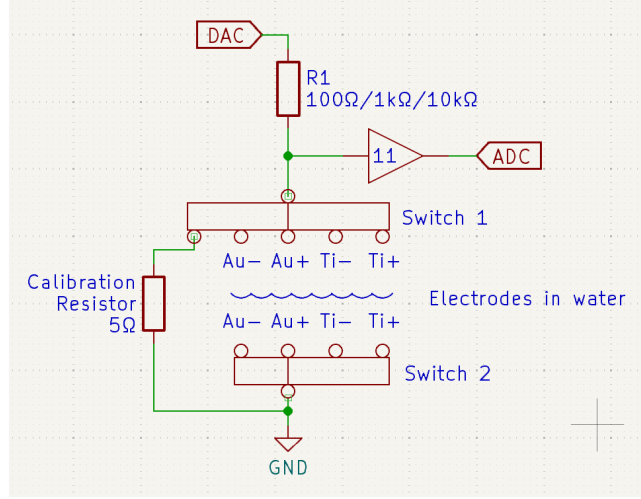


Figure 4.2: A simplified representation of the resistance measuring circuit.

titanium electrodes. The resistance across the titanium electrodes remained uncertain and thus, in addition to the varied spacing and electrode length, alternative resistor values for  $R_1$  were provided which could be selected using solder jumpers on the device.

The  $R_1$  values were chosen to be  $100\Omega$ ,  $1k\Omega$  and  $10k\Omega$  which would be used when the resistance between the probes is  $1\Omega - 10\Omega$ ,  $10\Omega - 100\Omega$  and  $100\Omega - 1k\Omega$  respectively. This would allow for a minimum resolution of 11% of  $V_{CC}$  for the voltage measurement by the [Analogue to Digital Converter \(ADC\)](#) as shown by Equation 4.2.

$$\frac{1\Omega}{1\Omega + 100\Omega} * 11 = 11\% \quad \frac{10\Omega}{10\Omega + 100\Omega} * 11 = 100\% \quad (4.2)$$

Switch 1 allows  $R_1$  to be connected to any of the four electrodes or a calibration resistor of  $5\Omega$  and switch 2 allows for the other electrode to be connected to ground. For example, switch 1 could be connected to Ti+ and switch 2 could be connected to Ti- to measure the resistance between the titanium electrodes. This configuration also allows current to flow in both directions between electrodes which can prevent excessive build of chlorine gas or sodium electroplating on the electrodes by taking a resistance measurement in both directions in rapid succession.

In order to increase the measurement accuracy of the resistance, multiple high accuracy resistors were placed in series to attain the values of  $R_1$  and the calibration resistor as this decreases the uncertainty of their resistance. This decreases the total uncertainty  $\delta_{R_{total}}$  by a factor of the number of parallel resistors  $n$  compared to the individual resistor uncertainty  $\delta_R$  as shown by Equation 4.3 to Equation 4.5.

$$[h]R_{total} = \left[ \sum_{i=1}^n \frac{1}{R} \right]^{-1} = \left( \frac{n}{R} \right)^{-1} = \frac{1}{n} \cdot R \quad (4.3)$$

$$[h] \text{ for a function } f(x_1, x_2, \dots, x_n), \text{ its uncertainty } \delta_f = \sqrt{\sum_{i=1}^n \left( \frac{\partial f}{\partial x_i} \delta x_i \right)^2} \quad (4.4)$$

$$[h] \therefore \delta_{R_{total}} = \sqrt{\left( \frac{\partial R_{total}}{\partial R} \delta_R \right)^2} = \sqrt{\left( \frac{1}{n} \delta_R \right)^2} = \frac{1}{n} \delta_R \quad (4.5)$$

The resistances for  $R_1$  were made from 3 parallel resistors with tolerance  $\pm 1\%$  giving a total uncertainty of  $\pm 0.3\%$  and the calibration resistor was made from 4 parallel resistors with tolerance  $\pm 1\%$  giving a total uncertainty of  $\pm 0.25\%$ .

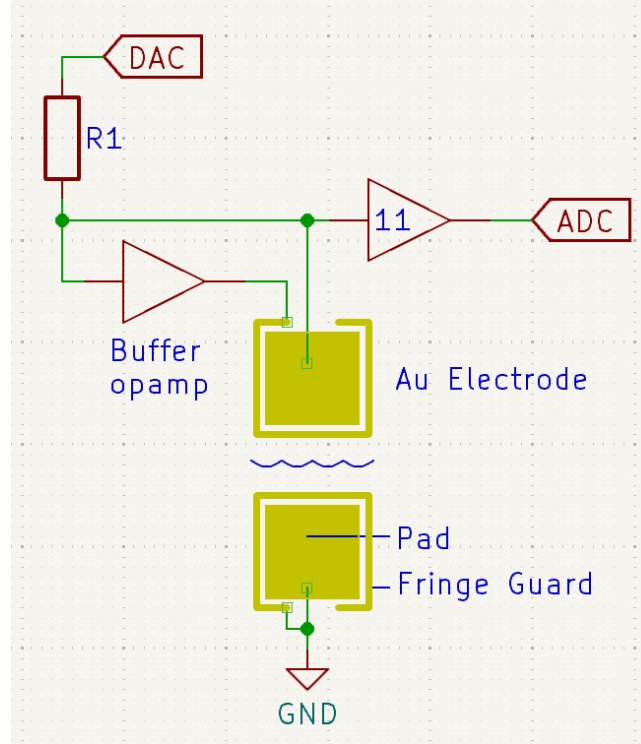


Figure 4.3: A simplified representation of the resistance measurement circuit using the gold electrodes with the fringe guard.

Figure 4.3 shows an example switch configuration where the gold electrodes are used. The buffer op-amp has unity gain and is used to repeat the voltage going to the pad of the top electrode to its fringe guard while the other pad and fringe guard are connected to ground. In theory, this should allow for the fringing to be absorbed by the fringe guard and not affect the resistance measurement, however switches were added electrically connect or disconnect the fringe guard should it interfere with the resistance measurement. The current flowing between the fringe guards was assumed to be less than that of the pads and thus there was no need to limit the current from the op-amp.

## 4.6 Salinity Calculation and Display

In order to measure the salinity of the sea ice, the probe needed to be lowered into the water and measure salinity at various depths. There are two methods for capturing the salinity data: either to constantly record the salinity data as the device is lowered through the water column or to have the device take a measurement when instructed by a controller. The former method creates logistical problems with waterproofing the device and retrieving data while the latter was a more user-friendly approach allowing researchers to control exactly which depths the salinity is measured at and was chosen for this project.

The controller consisted of a PCB with input buttons and two output 7-segment displays to control

and relay salinity information, and a RS485 communication port and a simple microcontroller. The RS485 communication port was chosen as the communication protocol as RS485 has the longest range and a high noise resistance which is necessary for the device to be used in the ocean which has high [Electromagnetic Interference \(EMI\)](#). The microcontroller was arbitrarily chosen from the STM32F030 series as it was relatively cheap, and it did not need to perform any complex calculations.

With an external controller, a waterproofed probe could be lowered into the water and measure the water's salinity. The chosen method of making a waterproof probe was to create a [PCB](#) and coat it with a layer of epoxy resin to waterproof it as this was the most familiar and cost-efficient method available. The probe [PCB](#) was designed with the equipment necessary to measure the salinity including ports for the conductivity probes, the circuitry required to measure the resistance as shown in Figure 4.2, temperature and depth sensors which are discussed in Section 4.7, an RS485 communication port and a microcontroller. The microcontroller that was chosen was from the STM32F401 series as STM microcontrollers as it had a [Floating Point Unit \(FPU\)](#) which allowed for calculating salinity on the probe.

## 4.7 Temperature and Depth Measurement

Depth sensors that are waterproof are too expensive for this project's budget. However, there have been alternative approaches which use non-waterproof sensors that are isolated from the water using a flexible membrane that would allow the pressure to be transmitted to the sensor. This project included a depth sensor with the aim to use this method to measure the depth of the probe in the water, however it also included a method for the user to manually input the depth of the probe in the water using the controller should this method fail.

The temperature sensor used in this project was an arbitrarily chosen, surface mount temperature sensor that had high accuracy and a wide temperature range. The temperature sensor should be coated with a thin layer of epoxy resin to waterproof it as epoxy resin is a poor thermal conductor and thus a thinner layer would allow for a more accurate temperature measurement. The choice of microcontroller and pressure sensor also provided this board with two alternative temperature sensors with less accuracy, however they could be used in the event that the primary temperature sensor failed.

## 4.8 [PCB](#) Assembly and Corrections

## 4.9 Salinometer Code

The salinometer has to measure the resistance between the electrodes, calculate the conductivity from that and then measure the temperature and pressure to finally calculate the salinity. In order to do a resistance measurement, the salinometer can either perform a single measurement or a multiple measurement voltage sweep. In either case, a voltage is first loaded onto the [DAC](#) which is then routed through an  $R_1$  resistor, then through the calibration resistor and then to ground and the voltage is recorded. After that the [DAC](#) is then routed through an  $R_1$  resistor, then through a pair of electrodes and then to ground and the voltage is recorded.

Given that the calibration resistance is known at  $5\Omega \pm 0.25\%$ , the resistance between the electrodes



can be calculated using the ratio the measured voltages as shown in Equation 4.6.

$$\frac{V_{calib}}{V_{electrode}} = \frac{R_{calib}}{R_{electrode}} \quad (4.6)$$

Using this method allows for the device to nullify all scalar inaccuracies in the circuit including  $R_1$  uncertainty, DAC and ADC gain errors, and the op-amp gain error. This is because the voltage measurement for both the calibration resistor and the electrodes would have the same inaccuracies. This method is however still vulnerable to offset inaccuracies including DAC and ADC offset errors and the internal resistance of the switches.

Once the resistance between the electrodes is known, the conductivity can either be calculated using the known area and length of the water between the gold electrodes or the conductivity can be calculated by using a more complex model if the titanium electrodes are used as they are subject to the fringing effect. Measuring the temperature and pressure is a simple matter of reading the temperature sensor and the pressure sensor respectively which finally allows salinity to be calculated which can be performed on the salinometer microcontroller as it possesses an FPU.

## 4.10 Controller Code

The controller's primary goal is to request measurements and display the returned values to the user. However, once the probe is cast in epoxy resin it will become unprogrammable and thus the controller must also be able to configure the probe's settings. The parameters that the controller will need to adjust include the  $R_1$  resistance, the electrode type, whether to use the fringe shield or not, the voltage sweep range and steps and the number of ADC samples to average.

## Chapter 5

# Salinometer Evaluation and Testing

The PCB boards were delivered and tested. Some design errors were found which include using op-amps that were rated for 6V instead of 3V3, missing a connection between VDDA and VCC, and footprints errors with both the temperature sensor and depth sensor. The temperature sensor footprint was unable to be corrected, but the depth sensor could be corrected by flipping the depth sensor.

Once the circuitry was working and coded, the salinometer was tested. The testing was conducted in two phases. One phase before the probe was cast into epoxy resin and the other after the probe was cast into epoxy resin (section numbers?). A summary of these tests is shown in Table 5.1 and each test is discussed in further detail in the following sections.

The equipment used to verify these tests were a bench multimeter model Keysight U3401A which had voltage accuracy to 0.02% and resistance accuracy to 0.1%.

Table 5.1: A summary of the evaluation and testing of the salinometer.

| Test                             | Description                                                                           | Ideal Result | Measured Result |
|----------------------------------|---------------------------------------------------------------------------------------|--------------|-----------------|
| DAC Voltage Range                | The range of voltages that the DAC can output from $0V$ to $V_{DD} = 3.3V$            | $0 - 3.3V$   |                 |
| ADC Accuracy                     | The average accuracy of the ADC in measuring voltages from $DAC_{MIN}$ to $DAC_{MAX}$ | 100%         |                 |
| Calibration Resistance           | The resistance of the calibration resistor $R_{CAL}$                                  | $5\Omega$    |                 |
| Calibration Resistance using ADC | The resistance of the calibration resistor $R_{CAL}$ as measured using the ADC        | $5\Omega$    |                 |

Continued on next page

Table 5.1: A summary of the evaluation and testing of the salinometer. (Continued)

|                                                   |                                                                                                                                                                      |               |  |
|---------------------------------------------------|----------------------------------------------------------------------------------------------------------------------------------------------------------------------|---------------|--|
| Resistance Measuring Accuracy                     | The salinometer's average accuracy in measuring specific resistances                                                                                                 | 100%          |  |
| Linear Conductivity Measurement Au                | Whether the sample of salt water had linear conductivity throughout a range of voltages or not using the gold electrodes with no fringe shield                       | Non-linear    |  |
| Linear Conductivity Measurement Shielded Au       | Whether the sample of salt water had linear conductivity throughout a range of voltages or not using the gold electrodes with the fringe shield                      | Linear        |  |
| Linear Conductivity Measurement Ti                | Whether the sample of salt water had linear conductivity throughout a range of voltages or not using the titanium electrodes                                         | Non-Linear    |  |
| Titanium Voltage to Conductivity Mapping Accuracy | How accurately the relationship between the voltage output by the DAC and the voltage measured over the titanium electrodes can correlate to a specific conductivity | 100% accuracy |  |
| Salinity Measurement Accuracy                     | The salinometer's average accuracy in measuring salinity                                                                                                             | 100%          |  |

## 5.1 DAC Voltage Range

The DAC configuration uses a transistor in order to buffer the DAC output which allows for the power draw to be support by the transistor instead of the DAC. This is a common configuration where the

DAC is connected to the non-inverting input of an op-amp whose output is connected to the base of an NPN transistor. The emitter of the transistor is then connected to the inverting input of the op-amp which allows the buffered output to match the input of the DAC.

This configuration does have one disadvantage in that the output voltage of the DAC is limited by the transistor's  $V_{BE}$  such that the highest voltage output at the emitter of the transistor is  $V_{DD} - V_{BE}$ . According to the transistor's data sheet, the buffered output should be limited to  $3.3V - 0.6V = 2.7V$  when conducting  $0A$  and  $3.3V - 0.75V = 2.55V$  when conducting the maximum current of  $33mA$  when the load is  $100\Omega$ . In order to assess the range and accuracy of the DAC, the DAC was instructed to output voltages from  $0V$  to  $V_{DD}$  in intervals of 64-bits and the output voltage was measured at the base and emitter of the buffer transistor and under maximum load of  $100\Omega$  and no load.  $V_{DD}$  and  $GND$  were measured to be  $3.299V$  and  $0V$  respectively.

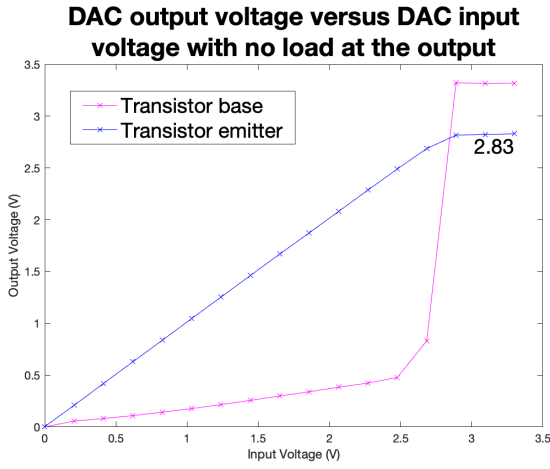


Figure 5.1: The input voltage versus the output voltage of the DAC with no load.

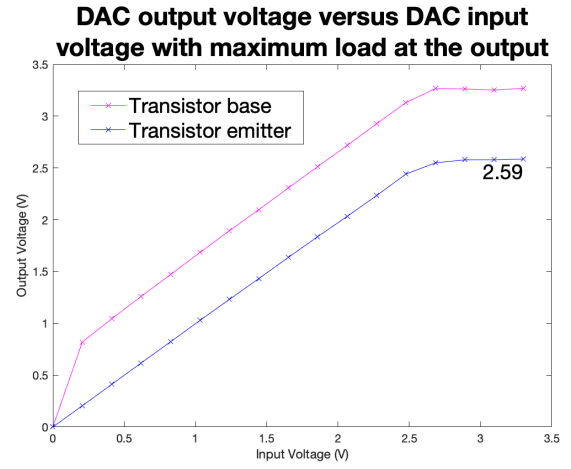


Figure 5.2: The input voltage versus the output voltage of the DAC with a load of  $100\Omega$ .

The results were graphed and are shown in Figure 5.1 and Figure 5.2. The voltage drop as a result  $V_{BE}$  can clearly be seen on Figure 5.2. The unloaded output voltage was able to reach  $2.83V$  and the loaded output voltage was able to reach  $2.59V$  which are slightly higher than the predicted limits.

An alternate attempt was also made to achieve a higher voltage output by using the internal reference voltage of the DAC. The internal reference voltage was set to  $4 \times 1.21V = 4.84V$  and the DAC was instructed to output the maximum voltage. As expected, this was not able to increase the output voltage; the base of the transistor still outputted  $3.3V$  and the emitter still outputted  $2.83V$  while unloaded.

Due to the voltage limitations, the DAC will have a limited output in future testing and implementation to prevent the output voltage not reaching the desired input voltage. The output will be limited to  $0V$  to  $2.5V$  or  $0$  to  $775$  for fully loaded tests and the implementation and  $0V$  to  $2.7$  or  $0$  to  $837$  for unloaded tests. When excluding the voltage readings above  $2.5V$ , the DAC was able to achieve a gain of  $0.9837V/V$  and an offset  $+0.0070V$  between the input voltage and output voltage when under maximum load.

*add LSB error = 0.00032V*

## 5.2 ADC Accuracy

The ADC will be tested by measuring a range of voltages produced by the DAC and comparing the voltage measured by a multimeter to the voltage measured by the ADC. The ADC will be configured in 12-bit mode with each measurement taking 15 ADC clock cycles and 5 measurements will be taken and averaged to increase the accuracy of the measurement. The accuracy of the ADC should ideally be 100%.

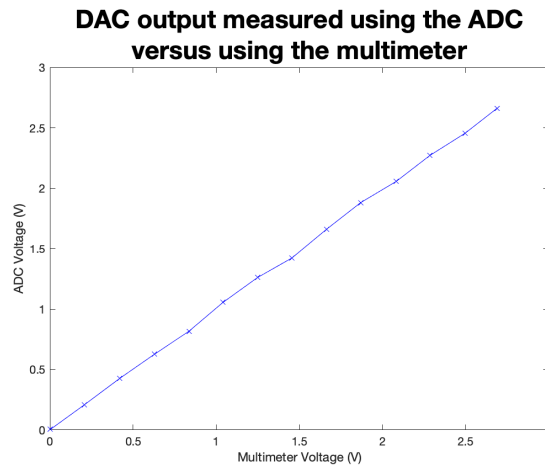


Figure 5.3: The voltage output by the DAC measured by a multimeter versus measured by the ADC.

The results are shown in Figure 5.3. The ADC achieved a gain of  $0.9877V/V$  and an offset of  $0.0082V$  when compared to the multimeter.

## 5.3 Calibration Resistance

The calibration resistor will be measured by using the multimeter and by using the ADC with and without the gain applied. The calibration resistance was specified to be  $5\Omega \pm 0.25\%$ , and thus it is expected to be between  $4.9875$  and  $5.0125\Omega$ .

The calibration resistors were electrically disconnected, and the multimeter was used to measure the calibration resistor to be  $5.25\Omega$  when the probes were applied directly across one of the parallel calibration resistor's terminals. The multimeter cables measured  $0.25\Omega$  when connected to each other and thus the final resistance of the calibration resistor was  $5.00\Omega$ . It should be noted that the multimeter could only measure down to  $0.01\Omega$  and thus the true resistance could range from  $4.99\Omega$  to  $5.01\Omega$ .

## 5.4 Resistance Measuring Accuracy

The method of measuring resistance involves getting a voltage reading of the calibration resistor and a sample resistor which is attached between the titanium electrode ports. The resistance of the sample resistor is then calculated using the ratio between the voltage across the sample resistor and the calibration resistor.

This will be done using two methods: one with a single voltage from the DAC of  $V_{DD}/2 = 1.65V$

and one with a range of voltages from the DAC with 50 samples. It was noticed during the testing phase that low voltage readings were not accurate as single bit errors caused large changes in the resistance reading and thus the range of voltages will be limited to  $0.3V$  to  $2.6V$  or 93 to 806 bits. Both measurements will then be compared to the resistance measured by the multimeter. The range of the resistors used will be  $0\Omega$  to  $10\Omega$  as this is the expected range for the gold electrodes.

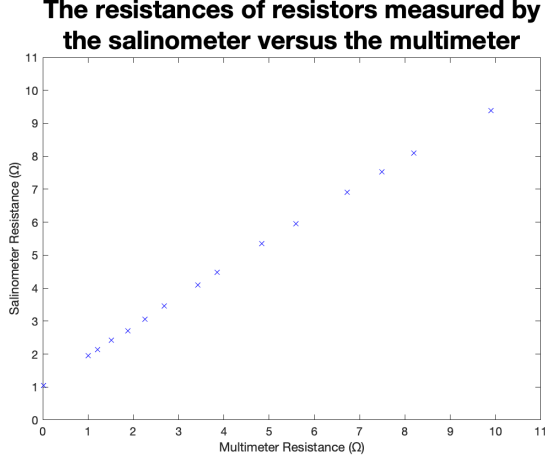


Figure 5.4: The resistance measuring test.

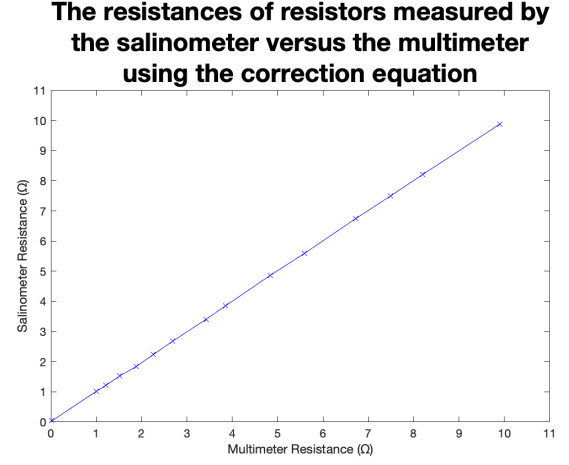


Figure 5.5: The resistance measuring test using the correction equation.

The results are shown in Figure 5.4 which shows that there is an error between the actual resistance and the resistance measured by the salinometer. This error was assumed to be due to the resistance of the switches and the traces. While these values could be measured and corrected for, a more effective method would be to generate a curve of best fit and use this to correct the resistance readings.

The equation for how the measured resistance  $R_{measured}$  was calculated is shown in Equation 5.1. This equation is then expanded using the resistor divider formula, then simplified and all the constant values are combined into the constants  $R_\alpha$ ,  $R_\beta$ , and  $K$  as shown in Equation 5.2. This equation is then rearranged to be a rational function using  $p$  and  $q$  coefficients which should give the equation of best fit for the data as shown in Equation 5.3.

$$R_{measured} = \frac{V_{resistor}}{V_{calibration}} \times R_{calibration} \quad (5.1)$$

$$\begin{aligned}
&= \frac{V_{DAC} A_{gain} \frac{R_{resistor} + r_{e1}}{R_{resistor} + R_1 + r_{e2}}}{V_{DAC} A_{gain} \frac{R_{calib} + r_{e3}}{R_{calib} + R_1 + r_{e4}}} \times R_{calibration} \\
&= \frac{R_{resistor} + r_{e1}}{R_{resistor} + R_1 + r_{e2}} \times \frac{R_{calibration}}{\left( \frac{R_{calib} + r_{e3}}{R_{calib} + R_1 + r_{e4}} \right)}
\end{aligned}$$

$$\begin{aligned}
R_{measured} &= \frac{R_{resistor} + R_{\alpha}}{R_{resistor} + R_{\beta}} \times K \\
&= \frac{K R_{resistor} + K R_{\alpha}}{R_{resistor} + R_{\beta}}
\end{aligned} \quad (5.2)$$

$$R_{measured} = \frac{p_1 R_{resistor} + p_2}{R_{resistor} + q_2} \quad (5.3)$$

The Equation 5.3 of best fit was confirmed using MATLAB giving  $p_1 = 87.3433$ ,  $p_2 = 92.3206$  and  $q_1 = 0.0001$ ,  $q_2 = 91.8310$  with an  $r^2$  value of 1.0000. Equation 5.3 could then be rearranged in terms of  $R_{resistor}$  to give the corrected resistance from the measured resistance  $R_{measured}$  as shown in Equation 5.4. After applying this equation to the recorded data, the results were graphed and are shown in Figure 5.5 with an  $r^2$  value of 1.0000.

$$R_{resistor} = \frac{p_2 - q_2 R_{measured}}{R_{measured} - p_1} \quad (5.4)$$

## Chapter 6

# Conclusions

The purpose of this project was to...

This report began with...

The literature review was followed in Chapter...

The bulk of the work for this project followed next, in Chapter...

In Chapter...

Finally, Chapter... attempted to...

In summary, the project achieved the goals that were set out, by designing and demonstrating...



## Chapter 7

# Recommendations

# Bibliography

- [1] *The Influence Of Formation Anisotropy Upon Resistivity - Porosity Relationships*, ser. SPWLA Annual Logging Symposium, vol. All Days, 06 1981.
- [2] T. E. S. Agency, “Mapping salty waters,” 2019. [Online]. Available: [https://www.esa.int/Applications/Observing\\_the\\_Earth/Space\\_for\\_our\\_climate/Mapping\\_salty\\_waters](https://www.esa.int/Applications/Observing_the_Earth/Space_for_our_climate/Mapping_salty_waters)
- [3] N. Snow and I. D. C. (NSIDC), “Ice sheet quick facts,” 2024. [Online]. Available: <https://nsidc.org/learn/parts-cryosphere/ice-sheets/ice-sheet-quick-facts>
- [4] R. H. Stewart, *Introduction to Physical Oceanography*. Texas A&M University Press, 2004. [Online]. Available: <https://www.uv.es/hegigui/Kasper/por%20Robert%20H%20Stewart.pdf>
- [5] R. F. HU Sverdrup, MW Johnson, *The Oceans, Their Physics, Chemistry, and General Biology*. New York: Prentice-Hall, 1942. [Online]. Available: <http://ark.cdlib.org/ark:/13030/kt167nb66r/>
- [6] E. L. Lewis and R. G. Perkin, “Salinity: Its definition and calculation,” *Journal of Geophysical Research*, vol. 83, no. C1, pp. 466–478, 1978. [Online]. Available: <https://agupubs.onlinelibrary.wiley.com/doi/epdf/10.1029/JC083iC01p00466>
- [7] Y. Zheng, Y. Liu, J. Zhou, and Y. Wang, “Electrical conductivity of the global ocean,” *Earth, Planets and Space*, vol. 69, no. 1, pp. 1–10, 2017.
- [8] E. B. editors, “Seawater,” *Encyclopædia Britannica*, 2024. [Online]. Available: <https://www.britannica.com/science/seawater>
- [9] W. S. Wooster, A. J. Lee, and G. Dietrich, “Redefinition of salinity,” *Journal of Marine Research*, vol. 27, no. 3, 1969.
- [10] U. G. Survey, “Water density,” 2018. [Online]. Available: [https://www.usgs.gov/special-topics/water-science-school/science/water-density#:~:text=A%20common%20unit%20of%20measurement,Celsius%20\(39.2Â°%20Fahrenheit\).](https://www.usgs.gov/special-topics/water-science-school/science/water-density#:~:text=A%20common%20unit%20of%20measurement,Celsius%20(39.2Â°%20Fahrenheit).)
- [11] B. Kjerfve, “Measurement and analysis of water current, temperature, salinity, and density,” in *Estuarine hydrography and sedimentation*, K. Dyer, Ed. Cambridge: Cambridge University Press, 1983, pp. 187–226.
- [12] U. of Washington Department of Oceanography, “A compilation of articles reporting research,” 1966.
- [13] H. Schmidt, S. Seitz, E. Hassel, and H. Wolf, “The density–salinity relation of standard seawater,” *Ocean Science*, vol. 14, no. 1, pp. 15–40, 2018. [Online]. Available: <https://os.copernicus.org/articles/14/15/2018/>

- [14] C. T. Swift and R. E. McIntosh, "Considerations for microwave remote sensing of ocean-surface salinity," *IEEE Transactions on Geoscience and Remote Sensing*, vol. GE-21, no. 4, pp. 480–491, 1983.
- [15] C. Gabarró, J. Font, A. Camps, M. Vall-llossera, and A. Julià, "A new empirical model of sea surface microwave emissivity for salinity remote sensing," *Geophysical Research Letters*, vol. 31, no. 1, 2004. [Online]. Available: <https://agupubs.onlinelibrary.wiley.com/doi/abs/10.1029/2003GL018964>
- [16] S. Yueh, R. West, W. Wilson, F. Li, E. Njoku, and Y. Rahmat-Samii, "Error sources and feasibility for microwave remote sensing of ocean surface salinity," *IEEE Transactions on Geoscience and Remote Sensing*, vol. 39, no. 5, pp. 1049–1060, 2001.
- [17] R. Millard and G. Seaver, "An index of refraction algorithm for seawater over temperature, pressure, salinity, density, and wavelength," *Deep Sea Research Part A. Oceanographic Research Papers*, vol. 37, no. 12, pp. 1909–1926, 1990. [Online]. Available: <https://www.sciencedirect.com/science/article/pii/019801499090086B>
- [18] D. Malardé, Z. Y. Wu, P. Grosso, J.-L. de Bougrenet de la Tocnaye, and M. L. Menn, "High-resolution and compact refractometer for salinity measurements," *Measurement Science and Technology*, vol. 20, no. 1, p. 015204, dec 2008. [Online]. Available: <https://dx.doi.org/10.1088/0957-0233/20/1/015204>
- [19] O. A. Tengesdal, "Measurement of seawater refractive index and salinity by means of optical refraction," Master's thesis, University of Bergen, 2012.
- [20] Y. Liao, K. Yang, and X. Shi, "Theoretical study on simultaneous measurement of seawater temperature and salinity based on dual fiber interferometers combined with nonlinear decoupling algorithm," *Measurement*, vol. 211, p. 112596, 2023. [Online]. Available: <https://www.sciencedirect.com/science/article/pii/S0263224123001604>
- [21] S. Yang, J. Xu, L. Ji, Q. Sun, M. Zhang, S. Zhao, and C. Wu, "In situ measurement of deep-sea salinity using optical salinometer based on michelson interferometer," *Journal of Marine Science and Engineering*, vol. 12, no. 9, 2024. [Online]. Available: <https://www.mdpi.com/2077-1312/12/9/1569>
- [22] G. R. C. Possetti, R. C. Kamikawachi, C. L. Prevedello, M. Muller, and J. L. Fabris, "Salinity measurement in water environment with a long period grating based interferometer," *Measurement Science and Technology*, vol. 20, no. 3, p. 034003, feb 2009. [Online]. Available: <https://dx.doi.org/10.1088/0957-0233/20/3/034003>
- [23] L. V. Nguyen, M. Vasiliev, and K. Alameh, "Three-wave fiber fabry–pérot interferometer for simultaneous measurement of temperature and water salinity of seawater," *IEEE Photonics Technology Letters*, vol. 23, no. 7, pp. 450–452, 2011.
- [24] Y. Zhao, J. Zhao, Y. Peng, R.-J. Tong, and L. Cai, "Simultaneous measurement of seawater salinity and temperature with composite fiber-optic interferometer," *IEEE Transactions on Instrumentation and Measurement*, vol. 71, pp. 1–8, 2022.

- [25] R. Somaraju and J. Trumpf, “Frequency, temperature and salinity variation of the permittivity of seawater,” *IEEE Transactions on Antennas and Propagation*, vol. 54, no. 11, pp. 3441–3448, 2006.
- [26] O. A. Tengesdal, B. L. Hauge, and L. E. Helseth, “Electromagnetic and optical methods for measurements of salt concentration of water,” *Journal of Electromagnetic Analysis and Applications*, vol. 6, no. 6, 2014.
- [27] S.-B. Scientific, “Conversion of pressure to depth,” 2024. [Online]. Available: <https://www.google.com/url?sa=t&rct=j&q=&esrc=s&source=web&cd=&ved=2ahUKEwU1sCIAxXPiv0HHXDELasQFnoECCMQAQ&url=https%3A%2F%2Fwww.seabird.com%2Fasset-get.download.jsa%3Fid%3D54627861710&usg=AOvVaw1fK2h9jmgpiBuyu8lkM1tl&opi=89978449>
- [28] I. O. Commission, “Teos-10: The international thermodynamic equation of seawater (teos-10) for temperature, salinity, density, sound speed, and other oceanographic variables,” *Manuals and Guides*, vol. 56, 2010. [Online]. Available: [https://www.teos-10.org/pubs/TEOS-10\\_Manual.pdf](https://www.teos-10.org/pubs/TEOS-10_Manual.pdf)
- [29] T. L. Hill, *An introduction to statistical thermodynamics*. Courier Corporation, 1986.
- [30] A. Poisson and M. H. Gadhoumi, “An extension of the practical salinity scale 1978 and the equation of state 1980 to high salinities,” *Deep Sea Research Part I: Oceanographic Research Papers*, vol. 40, no. 8, pp. 1689–1698, 1993. [Online]. Available: <https://www.sciencedirect.com/science/article/pii/096706379390022U>
- [31] G. T. Furukawa, J. L. Riddle, and W. R. Bigge, “The international practical temperature scale of 1968 in the region 13.81 k to 90.188 k as maintained at the national bureau of standards,” *Journal of Research of the National Bureau of Standards-A. Physics and Chemistry*, vol. 77A, no. 3, pp. 309–322, 1973. [Online]. Available: [https://nvlpubs.nist.gov/nistpubs/jres/77A/jresv77An3p309\\_A1b.pdf](https://nvlpubs.nist.gov/nistpubs/jres/77A/jresv77An3p309_A1b.pdf)
- [32] H. Preston-Thomas, “The international temperature scale of 1990 (its-90),” *Metrologia*, vol. 27, no. 107, pp. 3–10, 1990. [Online]. Available: [https://www.nist.gov/system/files/documents/pml/div685/grp01/ITS-90\\_metrologia.pdf](https://www.nist.gov/system/files/documents/pml/div685/grp01/ITS-90_metrologia.pdf)